Article

Photoaligning Polymeric Command Surfaces: Bind, or Mix?

Ameer R.K. Nassrah [1,2], Marianna Batkova [3], Natália Tomašovičová [3] and Tibor Tóth-Katona [1,*]

[1] Institute for Solid State Physics and Optics, Wigner Research Centre for Physics, P.O.Box 49, H-1525 Budapest, Hungary; tothkatona.tibor@wigner.hu
[2] Eötvös Loránd University, P.O.Box 32, H-1518 Budapest, Hungary
[3] Institute of Experimental Physics, Slovak Academy of Sciences, Watsonová 47, 04001 Košice, Slovakia; nhudak@saske.sk
* Correspondence: tothkatona.tibor@wigner.hu; Tel.: +36-1-392-2222 ext. 3623

Abstract: We compare photoaligning properties of polymer layers fabricated from the same constituents: polymethyl-methacrylate (PMMA) and azo-dye Disperse Red 1 (DR1), either chemically attached to the PMMA main-chain, or physically mixed with it. Photoaligning properties depend on the preparation method drastically. This finding is supported by atomic force microscope (AFM) scans monitoring the light-induced changes at the polymer−air interface, and revealing a photoinduced mass transfer.

Keywords: nematic–polymer interface; polymer–air interface; photoalignment; optical sensors; optical actuators

1. Introduction

Photoalignment of liquid crystals (LCs) [1–3] – discovered more than three decades ago [4–7] – can be achieved in contactless manner by proper light irradiation, and provides an alternative to standard aligning methods (such as, mechanical rubbing of polyimide layers), by which, in many cases the drawbacks and limitations of the rubbing method can be avoided. For example, in contrast to photoalignment, mechanical rubbing may produce and accumulate static charges and dust particles, can damage the alignment layer, can not align LCs in enclosed areas, or in microfluidic channels, etc. Since in these, photoaligning systems, very small number of photochromic derivatives anchored on a substrate commands the alignment of a very large number of LC molecules in contact with it, the surfaces were referred to as "command surfaces" [4].

Command surfaces are usually produced as monolayer of dye derivatives anchored on a substrate [4,8–12], or in the form of dye derivatives embedded in polymers and spin-coated on the substrate. In the latter case, prior the spin-coating, dye derivatives can be either physically mixed with (doped to) the polymer [5,7,13–16], or chemically attached to the polymer chain (in most cases by covalent bonding) [17–32].

In the above cited works azobenzene dye derivatives − exhibiting *trans-cis* (*E/Z*) isomerization [33] − have been used as photochromic units, due to their remarkable photo- and chemical stability, relative ease of synthesis, good solubility in liquid crystals (many azobenzene derivatives exhibit liquid crystalline properties themselves), and due to the reversibility of their polarization dependent photoisomerization. Namely, the polarised irradiation selectively excites the *trans* azo isomers depending on their orientation, and rapid successive *trans-cis-trans* isomerization cycles result in the orientation of the azobenzene long axis perpendicular to the light polarisation [33]. Nonetheless, other photochromic units, as well as other photoreactions are also exploited to implement photoaligning command surfaces, and are nicely summarized e.g., in Table 2 of Ref. [34]. As for the polymer host, in case of physical mixing with azobenzene derivatives, polyimide [5,7,14–16] and polyvinyl alcohol [13] has been used, while various azo-monomers have been chemically attached to the modified

main-chain of polyacrylates [29,30], polymethacrylates [20,21,25–28], polyamides [31], polyvinyl alcohols [17–19,22], or polysiloxanes [23,24].

The composition variety of the command surfaces in the above mentioned photoaligning systems largely prevents direct comparison of the benefits and disadvantages of the two fabrication methods (physical mixing/doping, and chemical binding). Moreover, our recent investigations [35–37] have shown that the mechanism and the efficiency of photalignment/photocontrol do not depend on the composition of the polymer layer exclusively, but also on the liquid crystal material in contact with the command surface. Therefore, for comparative investigations on the two systems, the use of the same polymer, same photochromic unit, and same liquid crystal compound is desirable. To the best of our knowledge, such a comparative investigation has not been reported yet, and one of the aims of the present work is to fill this gap. Nonetheless, the comparison of the photoalignment on command surfaces having disparate chemical composition allows us to notice some general trends. It seems that command surfaces prepared by physical mixing the polymer with the photochromic units requires significantly higher light power for photoalignment, the dynamics of the photoalignment is slower, and is less complete (the angle of the photoalignment is less than that required by the light polarisation), when compared to the command surfaces made of polymers grafted with photochromic units − see, e.g., in Ref. [38].

The second aim of the present work regards the investigations on the photoinduced mass transfer [39,40]. Namely, when the layer of a polymer grafted with azobenzene derivative is illuminated with a sinusoidal intensity pattern (obtained from the interference of two coherent laser beams), a large scale modulation of the free surface is obtained [41–43], which is referred to as surface relief gratings (SRG). The amplitude of the modulations has been found of the order of 100 nm, and the periodicity of the grooves was matching the periodicity of the illuminating interference pattern. Similarly, when the surface of the azobenzene-containing polymer film is irradiated with a single Gaussian laser beam with a radius focused down to few μm, a crater is formed, due to the photoinduced mass transfer [44,45]. Although, the mechanism with which the molecular *trans-cis-trans* cyclic photoisomerization converts to a macroscopic mass transfer is still under debate, the dependence of the created surface reliefs on the spatial modulation of the light intensity and on the light polarization is known [40].

In the present work, we do not produce interference pattern resulting in SRG, nor we focus the Gaussian laser beam to create a crater with radius of the order of μm, but rather we expand the laser beam to obtain photoalignment over a considerably large area (with a diameter of few millimeters). However, the question, how the photoaligning illumination modifies the free surface of the polymer, and whether a photoinduced mass transfer is detectable under these conditions, is still relevant.

As a final remark, we note here that SRG formation has already been investigated on the same systems [polymethyl-methacrylates (PMMA) doped-, or functionalized with Disperse Red 1 (DR1) dye] [46], as we consider in the present work. The formation of SRG has been found in both the DR1-doped PMMA system and in the DR1-functionalized polymer system, but the surface modulation was an order of magnitude larger in the latter case. Moreover, the surface grating effect was permanent only in the functionalized system.

2. Materials and Methods

For the experiments on photoalignment, liquid crystal cells of typical thickness $d \sim 10\mu$m have been prepared from a reference- and a photosensitive plate, into which the nematic liquid crystal mixture E7 [with the composition shown in Figure 1(c), and with the nematic-to-isotropic phase transition temperature $T_{NI} = 60$ °C] has been filled by capillary action. For the reference plate rubbed polyimide slide was used from E.H.C. Co. (Japan), which ensures a fixed, planar orientation of the liquid crystal at the surface (i.e., the director **n** is parallel with the surface of the plate). The photosensitive plates have been prepared by spin-coating on the glass substrate either the 2 wt% solution of polymethyl-methacrylate (PMMA) functionalized with Disperse Red 1 (DR1) dye [pDR1, Figure 1(a)], or the 2 wt% solution of the mixture PMMA+DR1 [Figure 1(b)] in toluene. Prior the

spin-coating, the glass substrates were cleaned by sonication, following the recipe of Ref. [47]: for 10 min in each of the following solvents in the order of ethanol, trichloroethylene, methylene chloride, ethanol again, rinsed by Millipore water (obtained by ELGA Purelab Option), and dried with a nitrogen jet. Spin-coating has been performed at 800 rpm for 5 s, and then at 3000 rpm for 30 s (all with spin acceleration of $\pm$1000 rpm/s). The spin-coated substrates have been baked in an oven for about 2 h at 140 °C. The thickness of the polymer layer has been estimated to be of the order of 0.1 μm, based on the spin-coating experiments on PMMA [47]. The reference and the photosensitive plates have been assembled with spacers, and the thickness of the assembled cells have been measured by interferometric method. Prior and during filling the cell with the LC mixture E7, it was illuminated with light polarized perpendicular to the rubbing direction on the reference plate.

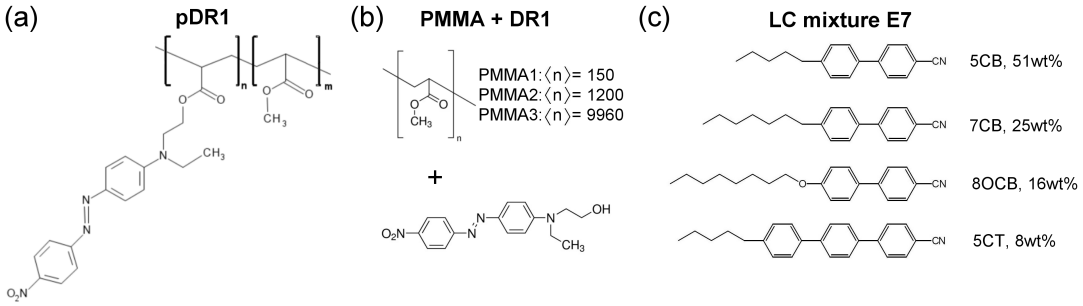

Figure 1. Molecular structures of (a) photosensitive polymer pDR1, n : m $\approx$ 1 : 9, (b) polymethyl-methacrylates (PMMA) of different number-average degree of polymerization $\langle$n$\rangle$ physically mixed the azo-dye Disperse Red 1 (DR1), and (c) the nematic liquid crystal mixture E7.

Mixtures PMMA+DR1 have been prepared with various PMMA polymers having different number-average degree of polymerization from $\langle$n$\rangle$ = 150 to $\langle$n$\rangle$ = 9960 as indicated in Figure 1(b), all obtained from Sigma-Aldrich and used as received. Namely, on one hand, the increase of the degree of polymerization increases the glass transition temperature (T_g) of PMMA [48,49]. On other hand, T_g in thin polymer films is known to influence the dynamic processes of other contacting materials, thus difference in T_g of the underlying polymer may substantially affect the photoalignment behavior of the layer [50]. For the midpoint of the glass transition temperature values of T_g = 105 °C and T_g = 125 °C have been given by the provider for PMMA1 and PMMA3, respectively [see Figure 1(b)], while for pDR1 [Figure 1(a)] a T_g = 119 °C has been measured [51]. In the photoalignment experiments, the content of DR1 in the mixture with PMMA has also been varied in a wide range: from 6.2 wt% of DR1 (that corresponds to the DR1 content of pDR1), up to 42 wt% of DR1.

The choice of the LC mixture E7 for further measurements on photoalignment is based on our previous studies. Namely, besides of the conveniently wide temperature range of the nematic liquid crystal phase (up to T_{NI} = 60 °C), at the interface with the pDR1 polymer layer, E7 showed the richest variety of photo-induced mechanisms compared to other nematic LC compounds [36,37]. At lower temperatures (close to room temperature) an almost complete azimuthal photoalignment is observable, achieved by a twist deformation, which relaxes back relatively fast upon switching off the exciting irradiation. In contrast, at high temperatures (close to T_{NI}) the azimuthal photoalignment vanishes, and instead, besides of a temperature induced anchoring transition, zenithal photoalignment occurs [35]. We have attributed this complex behaviour to different temperature dependence of the azimuthal and zenithal anchoring strengths [35], and to the molecular structure of the rigid core of E7 components that contain biphenyl, capable to establish $\pi - \pi$ aromatic interaction with the azo-benzene of pDR1 [36].

The pump-probe optical setup, combined with lock-in technique for the photoalignment measurements, as well as the methods for the determination of the *azimuthal* (in-plane) photoalignment angle, φ, and for the detection of the *zenithal* (out-of-plane) photoalignment have been described in details in Ref. [37]. The only difference between the measurement method presented here and those

reported in Refs. [35–37] is that for the determination of the *azimuthal* photoalignment angle, here, the polarization of the pump beam enclosed 45° with the initial director orientation **n** (instead of being parallel with it as in Refs. [35–37]). The reason for this change was to avoid accidental creation of a supertwist deformation in the LC cell [52]. Consequently, when switched on, the pump beam is expected to induce twist deformation in the LC cell with $\varphi = 45°$ at the photosensitive plate for the complete azimuthal photoalignment.

Atomic force microscopy (AFM) scans on the photosensitive substrates prior and after the polarized laser illumination were carried out with Agilent 5500 AFM system equipped by PicoView 1.14.3 control software. The images were acquired in the semi-contact (tapping) mode using medium soft silicon cantilevers (Oxford Instruments, model AC240TS-R3) with the resonant frequency of 70 kHz (typ.), and spring constant of 2 N/m (typ.). The measurements were performed at ambient relative humidity of $30 - 40\%$ at room temperature. The captured images were processed using freely available software from Gwyddion [53].

3. Results

3.1. Photoalignment measurements

In Figure 2 results on the *azimuthal* photoalignment/photoreorientation are shown, measured on LC cells with a photosensitive polymer layer from pDR1, as well as from PMMA1+DR1 mixture (with 30 wt% DR1 content) at a temperature $T_{NI} - T = 32$ °C, close to the room temperature. As we mentioned in Sect. 2, the polarization of the pump beam encloses 45° with the initial director orientation **n** at the reference plate.

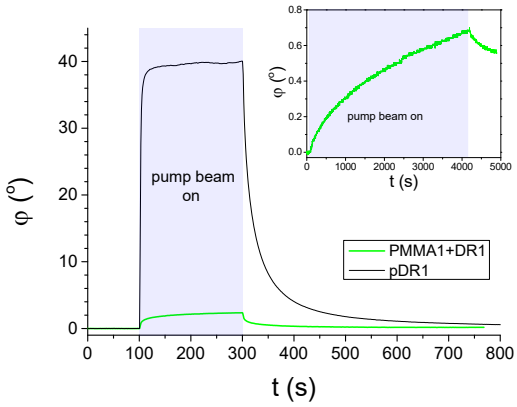

Figure 2. Azimuthal photo-reorientation angle φ in time, measured at temperature $T_{NI} - T = 32$ °C in cells filled with E7 and having pDR1, or PMMA1+DR1 mixture (with 30 wt% DR1 content) layer as a photosensitive plate. The pump-beam was switched on at $t = 100$ s, and switched off at $t = 300$ s. The power of the pump beam was $P = 10$ mW in case of the cell with pDR1, and $P = 70$ mW for the cell with PMMA1+DR1. Inset: long time illumination measurement on another location of the cell with PMMA1+DR1 (pump-beam switched on at $t = 100$ s, and switched off at $t = 4200$ s).

Results on the azimuthal photoalignment in the LC cell with pDR1 are in agreement with the previous results [35,36]: at low temperatures, upon light excitation, the azimuthal photoreorientation angle at the surface of pDR1 reaches a saturated value of $\varphi_{sat} \approx 40°$ relatively fast, *i.e.*, almost a complete azimuthal photoalignment occurs via photo-induced twist deformation in the LC layer. When the photo-excitation is switched off, a relatively fast back-relaxation is observed – the system returns to the initial, planar orientation.

In contrast, in the LC cell with the polymer layer from the PMMA1+DR1 mixture, upon the light excitation (despite of the much higher light power), a much smaller change in the azimuthal photoalignment angle has been observed (typically up to $\varphi \approx 3°$), and the small photo-induced change

does not seem to saturate even for long illumination times – see the inset of Figure 2. When the pump beam is switched off, the small photo-induced change in φ relaxes back slowly.

For the investigations on the *zenithal* photoalignment, the polarization of the probe beam has enclosed 45° with **n** (to maximise the sensitivity), while the polarization of the pump beam has been set perpendicular to **n**, which ensures the absence of the azimuthal photoalignment and its influence on the results. When significant zenithal photoalignment occurs, due to the change in the birefingence, oscillations appear in the transmitted light intensity of the probe beam when the pump beam is switched on/off. The results on zenithal photoalignment are shown in Figure 3 for two (low and high) temperatures, and for both cells with pDR1 and PMMA1+DR1.

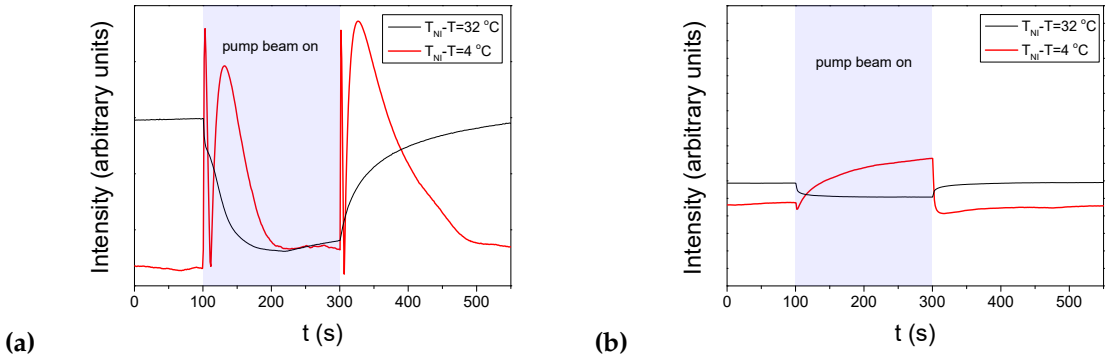

Figure 3. Temporal variation of the transmitted light intensity of the probe beam measured in E7 cells at two different temperatures in the setup for detection of zenithal photo-reorientation (pump beam polarization perpendicular to **n**, probe beam polarization encloses 45° with **n** – for the details of experimental setup refer to [37]). The pump-beam of power P switched on at $t = 100$ s, and switched off at $t = 300$ s. **(a)** pDR1, $P = 10$ mW; **(b)** PMMA1+DR1 mixture (with 30 wt% DR1 content), $P = 70$ mW.

Again, results on the zenithal photoalignment in the LC cell with pDR1 [Figure 3(a)] are in agreement with the previous results [35]: at low temperatures, upon irradiation, only a slight change in the transmitted light intensity has been observed, indicating the absence of zenithal photoalignment; at high temperatures, however, oscillations in the transmitted light intensity, both when pump beam is switched on and off, clearly indicate a significant zenithal photoalignment. In the analysis of Ref. [35], the zenithal photoalignment angle has been estimated to be in the range between $\theta_{photo} = 33°$ and $\theta_{photo} = 42.5°$.

In contrast, in the LC cell with the polymer layer from the PMMA1+DR1 mixture, upon the light excitation (despite of the much higher light power), only a slight change in the transmitted light intensity of the probe beam has been observed in the whole temperature range (from room temperature, up to T_{NI}) – see Figure 3(b). This slight change at all temperatures, may originate either from a small misalignment of the director at the two bounding surfaces, or from a small misalignment of the polarization direction of the pump beam and **n**, or eventually, from a slight zenithal photoalignment as it was discussed in Ref. [35].

We note here, that in the photoalignment measurements presented above, only the results on the mixture of PMMA1 [with the smallest $\langle n \rangle$ – see Figure 1(b)] with 30 wt% DR1 are shown. Other polymer layers have also been prepared from the mixtures of PMMA1, PMMA2, or PMMA3 with DR1 in different concentrations (with DR1 content ranging from 6.2 wt% to 42 wt%). Photoalignment measurements on LC cells with these substrates has led to essentially same results as those presented in Figures 2 and 3(b). Therefore, it seems that the photoaligning properties of polymer layers composed of the PMMA and DR1 mixture do not depend substantially on the degree of polymerisation, nor on the concentration of the photochromic material.

3.2. *Atomic force microscopy (AFM) on photosensitive substrates*

Previous investigations [36,37] have shown that at the pDR1 surface, the relatively fast back-relaxation of the azimuthal photoalignment angle φ when the exciting illumination is switched off (as shown in Figure 2), happens only when the pDR1 surface interfaces LC material having biphenyl in its rigid core. When pDR1 is in contact with LCs not having biphenyl in the molecular structure, there is no back-relaxation, or it is extremely slow. Therefore, it is reasonable to expect, that the pDR1 surface in contact with the air will not relax back on the time scales of hours after the exciting illumination. This assumption was a prerequisite for the AFM measurements presented in this subsection.

Glass substrates with pDR1 and with PMMA1+DR1 mixture (having 35 wt% DR1 content) have been prepared identically as those for photoalignment measurements. AFM scans were performed at certain (identical) locations prior and after the illumination with polarised light having intensity of the order of 100 mW/cm^2 (at $\lambda = 405$ nm).

AFM scans on the pDR1 substrate are shown in Figure 4 prior [(a) and (c)], and after [(b) and (d)] the illumination. The polarization direction of the illumination was set vertical (along the y direction).

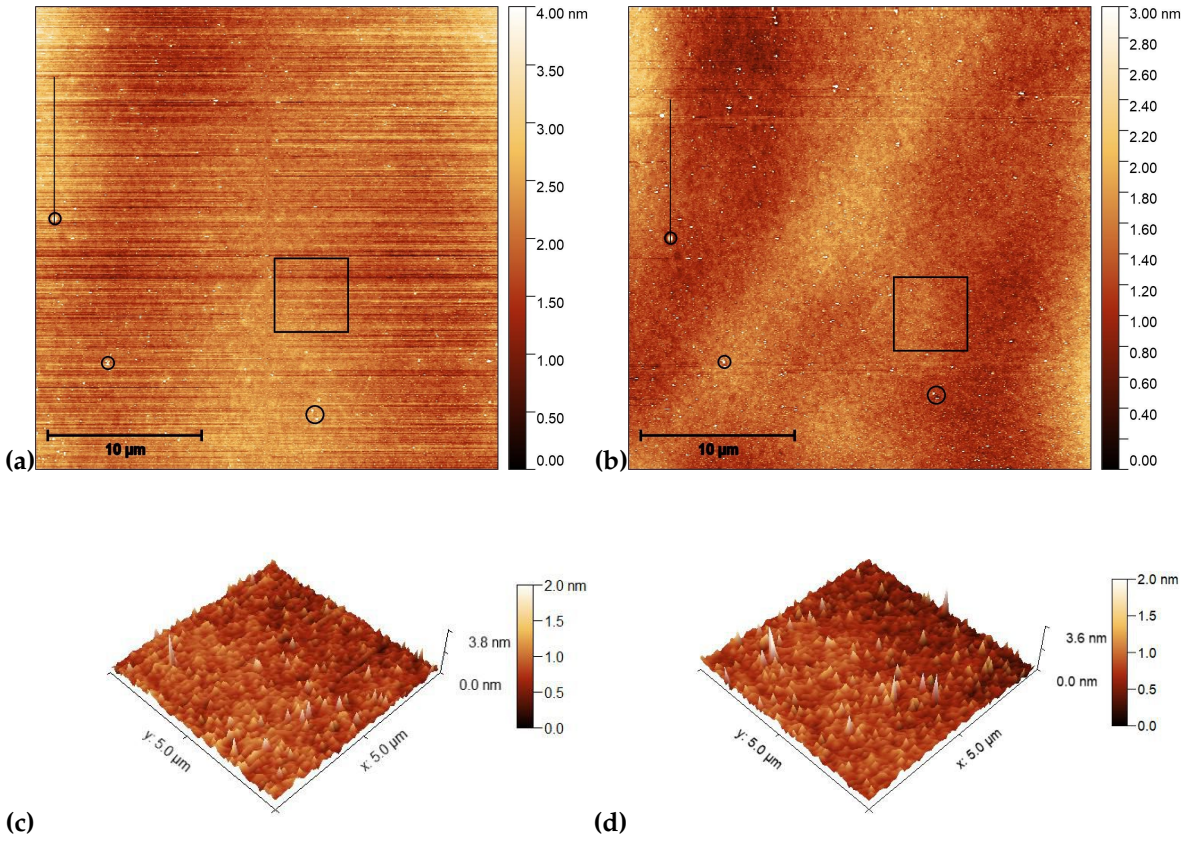

Figure 4. AFM images taken on the pDR1 surface prior [**(a)** and **(c)**], and after [**(b)** and **(d)**] the laser illumination. Encircled spots in **(a)** and **(b)** serve as reference locations to identify the same area for AFM scanning prior and after the illumination, while the squares denote the area that are presented in **(c)** and **(d)** in three dimensions. The vertical lines in **(a)** and **(c)** denote the locations from which the one dimensional profiles shown in Figure 7**(a)** are taken.

For the determination of the influence of the illumination it is critical to compare the same area of the substrate before and after the irradiation. For that purpose, reference locations have been selected which can be undoubtedly identify both prior and after the irradiation. Those locations are marked with black circles in Figure 4(a) and (b). One can see some photoinduced changes immediately from the AFM scans. First, changes in the surface relief: horizontal grooves (along x-axis) present prior the illumination (presumably caused by the spin-coating) [Figure 4(a) and (c)], disappear after

the illumination [Figure 4(b) and (d)]. The relative positions of the reference locations have slightly changed [*cf.* the positions of the locations marked with black circles in Figure 4(a) and (b)]. A closer look at the enlarged images shown in Figure 5 proves that even within the original reference location (black circle) the two white spots change their relative positions upon the irradiation. These are strong indications of the photoinduced mass transfer, and therefore, the selection of the area for the three-dimensional representation, shown in Figure 4(c) and (d), was based on new reference locations that do not change their relative positions upon illumination [indicated by yellow circles in Figure 5(a) and (b)].

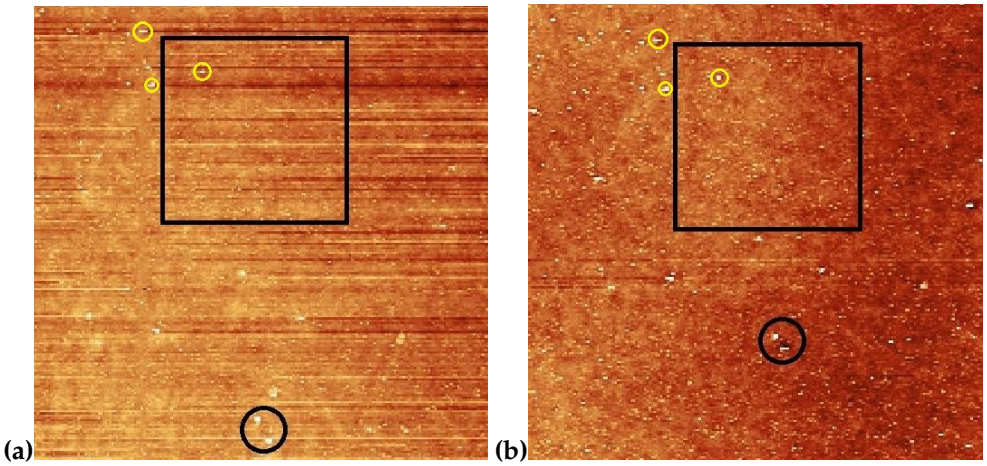

Figure 5. Enlarged images of the neighborhood of squares shown in Figure 4**(a)** and **(b)** with the new reference locations encircled with yellow; **(a)** prior the laser illumination; **(b)** after the illumination.

AFM scans on the PMMA1+DR1 substrate are shown in Figure 6 before [(a) and (c)], and after [(b) and (d)] the illumination. Again, the polarization direction of the illumination was set vertical (along the y direction). Here, no obvious photoinduced change is detectable.

A more detailed information about the photoinduced changes can be obtained from one dimensional profiles presented in Figure 7, taken along the lines shown in Figures 4 and 6, before and after the laser illumination.

One dimensional profiles taken on the pDR1 substrate along the line indicated in Figure 4(a) and (b) are shown in Figure 7(a). As a starting point ($y = 0$) for the profiles, one of the reference points − the high peak encircled in Figure 4(a) and (b) has been used. Obviously, the illumination smoothens the $z(y)$ profile: the roughness of $z(y) \approx \pm 0.5$ nm evidently becomes smaller after the illumination. In the same time, the smoothing causes a significant lateral photoinduced mass transfer too: for example, the high peak at $y = 3.2$ μm prior the illumination has moved to the position $y = 3.7$ μm after the illumination.

One dimensional profiles taken on the PMMA1+DR1 substrate along the line indicated in Figure 6(a) and (b) are shown in Figure 7(b). Here, the changes in the profile after the illumination are minimal, and are very close to the resolution of the AFM. The peaks and valleys undergo only slight changes upon illumination, and can be well identified individually before and after the illumination. Note that the last double peak at $x \approx 2.4$ μm shifts laterally by about 40 nm upon illumination, which is more than an order of magnitude smaller shift than that observed on pDR1 substrate, indicating a very small light induced mass transfer compared to that in pDR1.

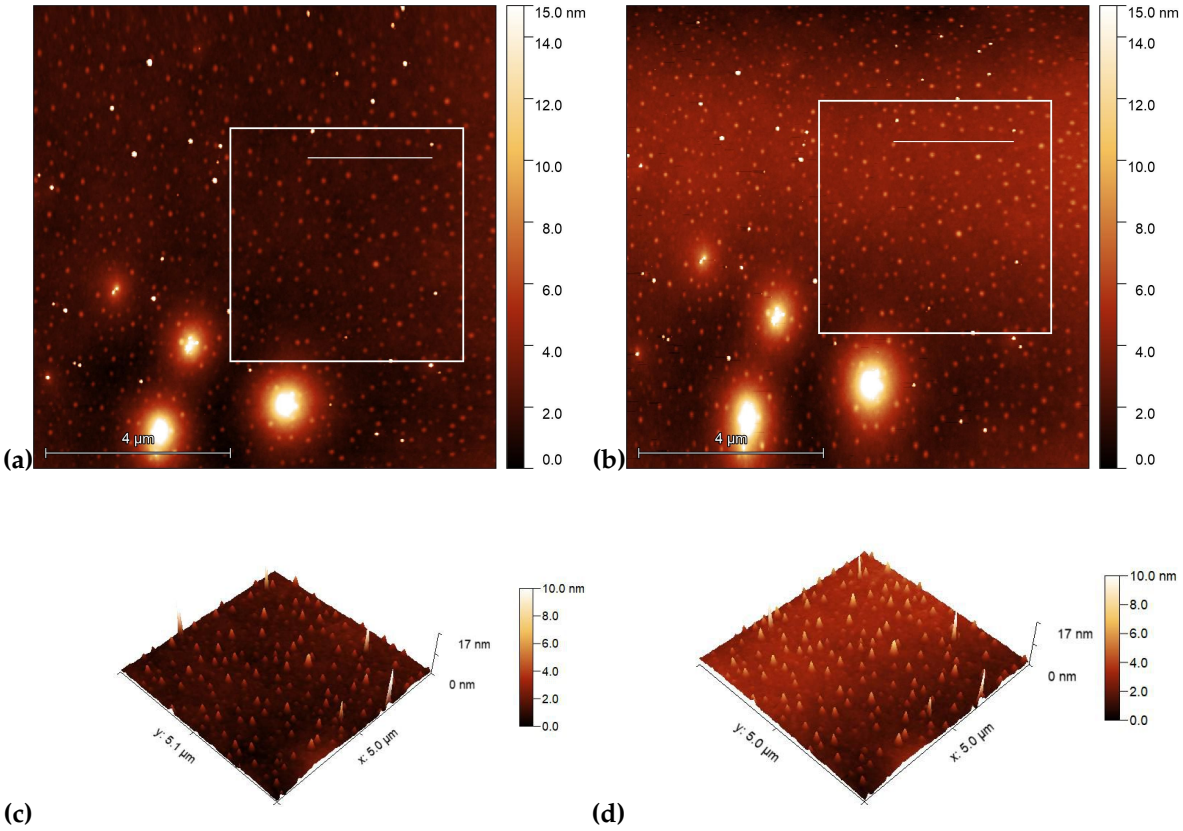

Figure 6. AFM images taken on the surface of PMMA1+DR1 mixture (with 35 wt% DR1 content) prior [**(a)** and **(c)**], and after [**(b)** and **(d)**] the laser illumination. The squares in **(a)** and **(b)** denote the area that are presented in **(c)** and **(d)** in three dimensions, while the horizontal lines in squares denote the locations from which the one dimensional profiles shown in Figure 7**(b)** are taken.

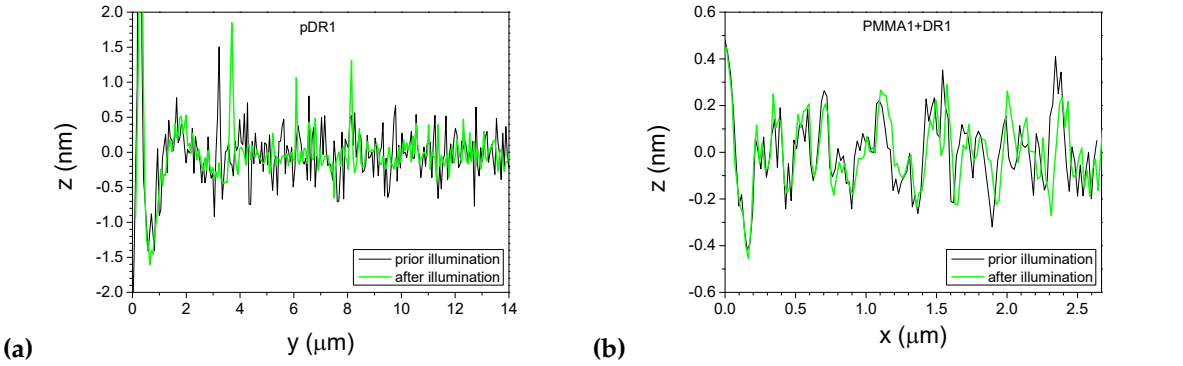

Figure 7. One dimensional profiles along the lines shown in Figures 4 and 6, taken before and after the laser illumination; **(a)** pDR1; **(b)** PMMA1+DR1.

4. Discussion

Photoalignment measurements on LC cells with a pDR1 substrate and with E7 nematic LC mixture have confirmed our previous results [35,36] concerning both the azimuthal and the zenithal photoalignment. In contrast to that, measurements on LC cells with various PMMA+DR1 substrates, filled with E7 have resulted in a very small, but measurable azimuthal photoalignment angles, while the zenithal photoalignment has been found negligible, if exists at all.

For the very weak photo-response measured in the LC cells with PMMA+DR1 substrates one can anticipate two possible reasons: **(i.)** the orientation of the DR1 molecules, and **(ii.)** the rigidity of the PMMA matrix.

Reason **(i.)** comes from both theoretical considerations and experimental data, evidencing that rod-like molecules often have a tendency to orient perpendicular to the free (air contacting) surface of the film [2]. Such an orientation of the azo-benzene derivatives is unfavorable for photoalignment when the light irradiation is performed (as in our case) with normal incidence to the film (substrate) plane, because this orientation results in poor light absorption. Assumption **(i.)** can be, however, tested by a slantwise illumination [25]. Namely, when illuminated with non-polarized light, the *trans* azo-benzene derivatives tend to reorient with their long axis in the direction parallel with the light propagation direction. Following the work of Ref. [25] we have tried to influence the initial orientation of DR1 molecules in the substrate made of PMMA1+DR1 mixture. In order to do that, after the preparation of the substrate from PMMA1+DR1 mixture, the polymer layer has been illuminated slantwise from a non-polarised $\lambda = (457 \pm 7)$ nm light source with illumination dose of 7.5 J/cm^2 and with light propagation direction which encloses 30° with the polymer film plane. The LC cell was than assembled, and prior as well as during filling the cell with E7, it was again illuminated with the same non-polarised light source in the same geometry with a dose of 7.5 J/cm^2. Such procedure is supposed to reorient long axis of DR1 molecules so that they enclose 30° with the polymer film plane, making the photoalignment experiments much more efficient. Photoalignment measurements on this LC cell, however, have led to results very similar to those shown in Figures 2 and 3(b).

Therefore, we assume that reason **(ii.)**, i.e., the rigidity of the PMMA matrix in the glassy state stays behind the poor photoalignment performance of the polymer layers made from PMMA+DR1 mixtures. Presumably, the rigid matrix hinders the cooperative motion (induced by the *trans-cis* isomerization of the DR1 molecules) necessary for an efficient photoalignment. In contrast to that, recently we have shown for a polymer segment of pDR1 that the trans-isomer of the azo-benzene moiety can take any direction at an energy expense of few *RT*, more likely due to the flexibility of the main chain than to the flexibility of the short spacer that connects the azo-dye with the polymer chain [37].

Results obtained from AFM scans on polymer reliefs in contact with the air are in line with the photoalignment measurements. The pDR1 surface evidently becomes smoother after the illumination, and the photoinduced changes in surface relief are accompanied with a significant photoinduced mass transfer. In contrast, the relief of PMMA1+DR1 surface does not change noticeably upon the illumination, and the photoinduced mass transfer has been found very close to the resolution of the AFM.

5. Conclusions

Results on the specific system presented in this work give a definite answer to the question posed in the title: the photoalignment is far more efficient when the azo-dye DR1 is chemically attached to the PMMA backbone, compared to the case when PMMA and DR1 are physically mixed. We attribute the poor photoalignment performance of the polymer layers prepared from PMMA+DR1 mixtures to the rigidity of the PMMA matrix.

The long-lasting (at least for *hours*, which follows from the timetable of the AFM measurements) photoinduced changes in the surface relief of pDR1, accompanied with significant photoinduced mass transfer support most of the results on photoalignment measurements at temperatures close to the room temperature. Namely, when in those measurements liquid crystals with phenylcyclohexane or bicyclohexane rigid core were contacting the pDR1 layer, extremely slow, or no back-relaxation occurred upon switching off the pump beam [36,37]. On the other hand, when LCs having biphenyl rigid core interface the pDR1 layer, the mechanisms of the fast back-relaxation shown in Figure 2 and reported in [35], as well as of the zenithal photoalignment at high temperatures shown in Figure 3(a) and in [35] still remain somewhat puzzling. AFM scans made at the pDR1 surface in contact with the air can not give insights on those mechanisms, presumably due to the absence of $\pi - \pi$ aromatic interaction between the contacting medium (air) and the azo-benzene of pDR1.

Author Contributions: Conceptualization, T.T.-K; methodology, T.T.-K, M.B. and N.T.; validation, A.R.K.N, M.B., N.T. and T.T.-K; formal analysis, A.R.K.N. M.B., N.T., and T.T.-K.; investigation, A.R.K.N. and M.B.; data curation, A.R.K.N., M.B. and T.T.-K.; writing–original draft preparation, T.T.-K.; writing–review and editing, A.R.K.N., M.B., N.T. and T.T.-K.; supervision, T.T.-K.; project administration, T.T.-K. All authors have read and agreed to the published version of the manuscript.

Funding: This research was funded by the National Research Development and Innovation Office (NKFIH) grant number FK 142643, and by the VEGA project No. 2/0043/21. A.R.K.N. acknowledges the financial support from Erasmus+ Programme, contract number 21/1/KA131/000003804/SMT-731, and the support obtained from Wigner RCP.

Acknowledgments: The polymer pDR1 was kindly provided by T. Kósa and L. Sukhomlinova (Alphamicron Inc., Kent OH, USA).

Conflicts of Interest: The authors declare no conflict of interest.

Sample Availability: The data presented in this study are available on request from the corresponding author.

References

1. Ichimura, K. Photoalignment in liquid-crystal systems. *Chem. Rev.* **2000**, *100*, 1847–1873.
2. Seki, T. New strategies and implications for the photoalignment of liquid crystalline polymers. *Polym. J.* **2014**, *46*, 751–768.
3. Bisoyi, H.K.; Li, Q. Light-driven liquid crystalline materials: From photo-induced phase transitions and property modulations to applications. *Chem. Rev.* **2016**, *116*, 15089–15166.
4. Ichimura, K.; Suzuki, J.; Seki, T.; Hosoki, A.; Aoki, K. Reversible change in alignment mode of nematic liquid crystals regulated photochemically by "command surfaces" modified with an azobenzene monolayer. *Langmuir* **1988**, *4*, 1214–1216.
5. Gibbons, W.M.; Shannon, P.J.; Sun, S.T.; Swetlin, B.J. Surface-mediated alignment of nematic liquid crystals with polarized laser light. *Nature* **1991**, *351*, 49–50.
6. Dyadyusha, A.G.; Marusii, T.; Reznikov, Y.; Khiznyak, A.; Reshetnyak, V. Orientational effect due to a change in the anisotropy of the interaction between a liquid crystal and a bounding surface. *JETP Lett.* **1992**, *56*, 17–21.
7. Gibbons, W.M.; Kósa, T.; Palffy-Muhoray, P.; Shannon, P.J.; Sun, S.T. Continuous grey-scale image storage using optically aligned nematic liquid crystals. *Nature* **1995**, *377*, 43–46.
8. Aoki, K.; Seki, T.; Suzuki, Y.; Tamaki, T.; Hosoki, A.; Ichimura, K. Factors affecting photoinduced alignment regulation of cyclohexanecarboxylate-type nematic liquid crystals by azobenzene molecular films. *Langmuir* **1992**, *8*, 1007–1013.
9. Seki, T.; Sakuragi, M.; Kawanishi, A; Tamaki, T.; Fukuda, R.; Ichimura, K. "Command surfaces" of Langmuir-Blodgett films. Photoregulations of liquid crystal alignment by molecularly tailored surface azobenzene layers. *Langmuir* **1993**, *9*, 211–218.
10. Ichimura, K.; Hayashi, Y.; Akiyama, H.; Ishizuki, N. Photoregulation of in-plane reorientation of liquid crystals by azobenzenes laterally attached to substrate surfaces. *Langmuir* **1993**, *9*, 3298–3304.
11. Yi, Y.; Farrow, M.J.; Korblova, E.; Walba, D.M.; Furtak, T.E. High-sensitivity aminoazobenzene chemisorbed monolayers for photoalignment of liquid crystals. *Langmuir* **2009**, *25*, 997–1003.
12. Jánossy, I.; Fodor-Csorba, K.; Vajda, A.; Palomares, L.O. Light-induced spontaneous pattern formation in nematic liquid crystal cells. *Appl. Phys. Lett.* **2011**, *99*, 111103/1–3.
13. Iimura, Y.; Kusano, J.; Kobayashi, S.; Aoyagi, T.; Sugano, T. Alignment control of a liquid crystal on a photosensitive polyvinylalcohol film. *Jpn. J. Appl. Phys., Part 2* **1993**, *32*, L93–L96.
14. Shannon, P.J.; Gibbons, W.M.; Sun, S.T.; Swetlin, B.J. Patterned optical properties in photopolymerized surface-aligned liquid-crystal film. *Nature* **1994**, *368*, 532–533.
15. Jánossy, I.; Jákli, A.; Nair, G.G.; Raina, K.K.; Kósa, T. Optical control of the alignment of a liquid crystal in the smectic A phase. *Mol. Cryst. Liq. Cryst.* **1999**, *329*, 507–516.
16. Jánossy, I.; Vajda, A.; Paksi, T.; Kósa, T. Photoinduced surface alignment: The role of the liquid crystalline order. *Mol. Cryst. Liq. Cryst.* **2001**, *359*, 157–166.

17. Ichimura, K.; Suzuki, Y.; Seki, T.; Kawanishi, Y.; Aoki, K. Reversible alignment change of a nematic liquid crystal induced by pendent azobenzene groups-containing polymer thin films. *Makromol. Chem., Rapid Commun.* **1989**, *10*, 5–8.
18. Kawanishi, Y.; Seki, T.; Tamaki, T.; Ichimura, K.; Ikeda, M.; Aoki, K. Reversible alignment change of nematic liquid crystals by photochromic polymer films. *Polym. Adv. Technol.* **1990**, *1*, 311–318.
19. Kawanishi, Y.; Tamaki, T.; Seki, T.; Sakuragi, M.; Suzuki, Y.; Ichimura, K.; Aoki, K. Multifarious liquid crystalline textures formed on a photochromic azobenzene polymer film. *Langmuir* **1991**, *7*, 1314–1315.
20. Ichimura, K.; Akiyama, H.; Ishizuki, N.; Kawanishi, Y. Azimuthal orientation of liquid crystals photo-controlled by an azobenzene pendent polymer. *Makromol. Chem., Rapid Commun.* **1993**, *14*, 813–817.
21. Akiyama, H.; Kudo, K.; Ichimura, K. Novel polymethacrylates with laterally attached azobenzene groups displaying photoinduced optical anisotropy. *Macromol. Rapid Commun.* **1995**, *16*, 35–41.
22. Akiyama, H.; Momose, M.; Ichimura, K.; Yamamura, S. Surface-selective modification of poly(vinyl alcohol) films with azobenzenes for in-plane alignment photocontrol of nematic liquid crystals. *Macromolecules* **1995**, *28*, 288–293.
23. Tang, Y.; Liu, D.; Xie, P.; Zhang, R. Photo-driven liquid crystal cell using azobenzene-grafted ladderlike polysiloxane as command layer. *Macromol. Rapid Commun.* **1996**, *17*, 759–766.
24. Tang, Y.; Xie, P.; Liu, D.; Zhang, R. Performance-improved photo-driven liquid crystal cell using azobenzene-grafted ladderlike polysiloxane as command layer. *Macromol. Chem. Phys.* **1997**, *198*, 1855–1863.
25. Ichimura, K.; Morino, S.; Akiyama, H. Three-dimensional orientational control of molecules by slantwise photoirradiation. *Appl. Phys. Lett.* **1998**, *73*, 921–923.
26. Ruslim, C.; Ichimura, K. Comparative studies on isomerization behavior and photocontrol of nematic liquid crystals using polymethacrylates with 3,3′- and 4,4′-dihexyloxyazobenzenes in side chains. *Macromolecules* **1999**, *32*, 4254–4263.
27. Ruslim, C.; Ichimura, K. Photocontrolled alignment of chiral nematic liquid crystals. *Adv. Mater.* **2001**, *13*, 641–644.
28. Palffy-Muhoray, P.; Kosa, T.; Weinan, E. Dynamics of a light driven molecular motor. *Mol. Cryst. Liq. Cryst.* **2002**, *375*, 577–591.
29. Ryabchun, A.V.; Bobrovsky, A.Yu.; Shibaev, V.P. Photoinduced reorientation processes in thin films of photochromic LC polymers on substrates with a photocontrollable command surface. *Polym. Sci. - A* **2010**, *52*, 812–823.
30. Bobrovsky, A.; Ryabchun, A.; Shibaev, V. Liquid crystals photoalignment by films of side-chain azobenzene-containing polymers with different molecular structure. *J. Photochem. Photobiol. A* **2011**, *218*, 137–142.
31. Ryabchun, A.; Bobrovsky, A.; Chun, S.-H.; Shibaev, V. A novel generation of photoactive comb-shaped polyamides for the photoalignment of liquid crystals. *J. Polym. Sci., Part A: Polym. Chem.* **2013**, *51*, 4031–4041.
32. Petrov, S.; Chau, N.H.M.; Marinova, V.; Sun, C.-C.; Hsu, K.-Y.; Lin, S.-H. Controllable LC anchoring on poly1-[4-(3-carboxy-4-hydroxyphenylazo) benzenesulfonamido]-1,2-ethanediyl, sodium salt command surface. *Polymer* **2023**, *272*, 125841/1–6.
33. Bandara, H.M.D.; Burdette, S.C. Photoisomerization in different classes of azobenzene. *Chem. Soc. Rev.* **2012**, *41*, 1809–1825.
34. Seki, T.; Nagano, S.; Hara, M. Versatility of photoalignment techniques: From nematics to a wide range of functional materials. *Polymer* **2013**, *54*, 6053–6072.
35. Tóth-Katona, T.; Jánossy, I. Photoalignment at the nematic liquid crystal-polymer interface: Experimental evidence of three-dimensional reorientation. *J. Mol. Liq.* **2019**, *285*, 323–329.
36. Nassrah, A.K.R.; Jánossy, I.; Tóth-Katona, T. Photoalignment at the nematic liquid crystal–polymer interface: The importance of the liquid crystalline molecular structure. *J. Mol. Liq.* **2020**, *312*, 113309.
37. Nassrah, A.K.R.; Jánossy, I.; Kenderesi, V.; Tóth-Katona, T. Polymer–nematic liquid crystal interface: On the role of the liquid crystalline molecular structure and the phase sequence in photoalignment. *Polymers* **2021**, *13*, 193/1–13.
38. Jánossy, I.; Tóth-Katona, T. Photo-orientation of liquid crystals on azo dye-containing polymers. *Polymers* **2022**, *14*, 159/1–12.
39. Shibaev, V.P.; Bobrovsky, A.Yu. Liquid crystalline polymers: Development trends and photocontrollable materials. *Russ. Chem. Rev.* **2017**, *86*, 1024–1072.

40. Oscurato, S.L.; Salvatore, M.; Maddalena, P.; Ambrosio, A. From nanoscopic to macroscopic photo-driven motion in azobenzene-containing materials. *Nanophotonics* **2018**, *7*, 1387–1422.
41. Rochon, P.; Batalla, E.; Natansohn, A. Optically induced surface gratings on azoaromatic polymer films. *Appl. Phys. Lett.* **1995**, *66*, 136–138.
42. Kim, D.Y..; Tripathy, S.K.; Li, L.; Kumar, J. Laser-induced holographic surface relief gratings on nonlinear optical polymer films. *Appl. Phys. Lett.* **1995**, *66*, 1166–1168.
43. Kim, D.Y.; Li, L.; Jiang, X.L.; Shivshankar, V.; Kumar, J.; Tripathy, S.K. Polarized laser induced holographic surface relief gratings on polymer films. *Macromolecules* **1995**, *28*, 8835–8839.
44. Bian, S.; Li, L.; Kumar, J.; Kim, D.Y.; Williams, J.; Tripathy, S.K. Single laser beam-induced surface deformation on azobenzene polymer films. *Appl. Phys. Lett.* **1998**, *73*, 1817–1819.
45. Bian, S.; Liu, W.; Williams, J.; Samuelson, L.; Kumar, J.; Tripathy, S. Photoinduced surface relief grating on amorphous poly(4-phenylazophenol) films. *Chem. Mater.* **2000**, *12*, 1585–1590.
46. Lagugné Labarthet, F.; Buffeteau, C.; Sourisseau, C. Analyses of the diffraction efficiencies, birefringence, and surface relief gratings on azobenzene-containing polymer films. *J. Phys. Chem. B* **1998**, *102*, 2654–2662.
47. Walsh, C.B.; Franses, E.I. Ultrathin PMMA films spin-coated from toluene solutions. *Thin Solid Films* **2003**, *429*, 71–76.
48. Thompson, E.V. Dependence of the glass transition temperature of poly(methyl methacrylate) on tacticity and molecular weight. *J. Polym. Sci. A2* **1966**, *4*, 199–208.
49. Ute, K.; Miyatake, N.; Hatada, K. Glass transition temperature and melting temperature of uniform isotactic and syndiotactic poly(methyl methacrylate)s from 13mer to 50mer. *Polymer* **1995**, *36*, 1415–1419.
50. Haque, H.A.; Hara, M.; Nagano, S.; Seki, T. Photoinduced in-plane motions of azobenzene mesogens affected by the flexibility of underlying amorphous chains. *Macromolecules* **2013**, *46*, 8275–8283.
51. DSC measurement has been performed at Alphamicron Inc., Kent OH, USA.
52. Jánossy, I.; Tóth-Katona, T.; Kósa, T.; Sukhomlinova, L. Super-twist generation and instabilities in photosensitive liquid crystal cells. *J. Mol. Liq.* **2018**, *267*, 177-181.
53. Available at: http://gwyddion.net (Accessed: 22 August 2023).